Received: 28 May 2020 | Revised: 18 September 2020 | Accepted: 25 September 2020

DOI: 10.1111/bcpt.13505

ORIGINAL ARTICLE

BCPT Basic & Clinical Pharmacology & Toxicology

Thal protects against paraquat-induced lung injury through a microRNA-141/HDAC6/IκBα-NF-κB axis in rat and cell models

Fenshuang Zheng[1] | **Junbo Zhu**[1] | **Wei Zhang**[1] | **Yangshan Fu**[1] | **Zhaoheng Lin**[2]

[1]Department of Emergency Medicine, Second People's Hospital of Yunnan Province, Kunming, China

[2]Department of Critical Care Medicine, People's Hospital of Xishuangbanna Dai Nationality Autonomous Prefecture, Pingpong, China

Correspondence
Zhaoheng Lin, Department of Critical Care Medicine, People's Hospital of Xishuangbanna Dai Nationality Autonomous Prefecture, No. 2, Gala South Road, Jinghong 666100, Yunnan, China.
Email: linzhaoH022501@163.com

Funding information
Key project of Kunming Science and Technology Plan: Basic and Clinical Study on Thalidomide in the Treatment of Paraquat Poisoning Lung Injury, Grant/Award Number: 2015-2-S-01408

Abstract

The protective functions of thalidomide in paraquat (PQ)-induced injury have been reported. But the mechanisms remain largely unknown. In this research, a PQ-treated rat model was established and further treated with thalidomide. Oedema and pathological changes, oxidative stress, inflammation, fibrosis and cell apoptosis in rat lungs were detected. A PQ-treated RLE-6TN cell model was constructed, and the viability and apoptosis rate of cells were measured. Differentially expressed microRNAs (miRNAs) after thalidomide administration were screened out. Binding relationship between miR-141 and histone deacetylase 6 (HDAC6) was validated. Altered expression of miR-141 and HDAC6 was introduced to identify their involvements in thalidomide-mediated events. Consequently, thalidomide administration alone exerted no damage to rat lungs; in addition it reduced PQ-induced oedema. The oxidative stress, inflammation and cell apoptosis in rat lungs were reduced by thalidomide. In RLE-6TN cells, thalidomide increased cell viability and decreased apoptosis. miR-141 was responsible for thalidomide-mediated protective events by targeting HDAC6. Overexpression of HDAC6 blocked the protection of thalidomide against PQ-induced injury via activating the IkBα-NF-κB signalling pathway. Collectively, this study evidenced that thalidomide protects lung tissues from PQ-induced injury through a miR-141/HDAC6/IkBα-NF-κB axis.

KEYWORDS

gene expression, lung injury, Paraquat, risk assessment, thalidomide, viability, Wistar rat

1 | INTRODUCTION

Paraquat (1,1-dichloro-4,4-bipyridine, PQ) is a widely used herbicide in agriculture and with extremely potent toxicity that leads to serious public health problem once misused.[1] By accidental or voluntary ingestion, PQ poisoning results in numerous deaths annually, mainly in developing countries where PQ is more largely used.[2] In oral ingestion cases, the mortality rate is over 90%.[3] PQ poisoning through oral, skin and respiratory tracts contributes to multiple organ failure including lungs, kidneys, liver and nervous system, in which the lung is the primary target organ.[4,5] This phenomenon was attributed to high affinity of PQ to alveolar cells.[6] Therefore, PQ poisonings usually cause acute lung injury and, ultimately, acute respiratory distress syndrome and death.[7] Unfortunately, despite the large volume of studies in the past

decades, there is no effective regimens for PQ poisoning treatment, leaving the clinical outcome largely depending on the degree of exposure.[6] Excessive oxidative damage and cell death caused by the release of superoxide anions in organisms[8] and inflammation in lung tissues are main contributors to high severity and mortality, and are also promising targets for clinal control for PQ-induced lung injury.

Thalidomide was first developed in 1957 and widely served as a sedative worldwide, but it was banned from the market soon in 1961 due to its side-effect of teratogenicity.[9] Despite this, thalidomide is a well-known immunomodulatory compound that has been noted as a potential drug for autoimmune diseases,[10] angiogenesis-related diseases including cancer[11] and inflammation control.[12,13] Importantly, the anti-inflammatory effect of thalidomide in PQ-induced pulmonary injury has been witnessed in a mouse model.[14] However, the molecules involved are largely unstudied yet. MicroRNAs (miRNAs) are a class of versatile non-coding RNAs that fulfil diverse functions in cellular behaviours and biological presentations including oxidative stress and inflammation.[15] miR-141, which was reported to alleviate lipopolysaccharide (LPS)-induced inflammation[16] in WI-38 fibroblasts, was found significantly upregulated after thalidomide treatment in this study. We then speculated that miR-141 is possibly involved in thalidomide-mediated events. In addition, histone deacetylase 6 (HDAC6) was identified as a target transcript of miR-141 in the present work. HDAC6 has been reported to be closely linked to inflammation and oxidative stress.[17,18] But its role in PQ-induced lung injury remains unclear. Besides, the inhibitor of kappa-B subunit alpha (IκBα)-nuclear factor kappa-B (NF-κB) signalling pathway is well-known to participate in innate immune responses and inflammation,[19] and it is also implicated in the progression of acute lung injury.[20] Collectively, we hypothesized that thalidomide protects lung against PQ-induced injury involving miR-141, HDAC1 and the IκBα-NF-κB signalling.

Animal models are frequently used in basic researches to study the function of drugs or molecules, and rats are frequently used as models of PQ-induced lung injury.[21,22] Besides, type II rat alveolar epithelial cells (RLE-6TN) are frequently used for in vitro studies in the toxicity of PQ.[23,24] Compared to the type I alveolar cell, type II cell has the potential of division, proliferation and differentiation into type I cells, and they can repair the damaged epithelium. Damage of type II alveolar cells may reduce the surfactant on alveoli, leading to lung oedema and respiratory distress, which is concert with the features of PQ-induced rats. Taken together, in this study, we used Wistar rats and RLE-6TN cells to establish PQ-induced models in vivo and in vitro, respectively, to determine the effects of PQ and thalidomide, and the potentially involved molecules in lung injury. The oedema in rat lung tissues was determined according to the ratio of wet to dry (W/D) weight. Haematoxylin and eosin (HE) staining was performed to observe the pathological changes. Enzyme-linked immunosorbent assay (ELISA), reverse transcription quantitative polymerase chain reaction (RT-qPCR) and Western blot assays were used to determine the expression of different molecules and cytokines, while apoptosis and viability of cells was detected by flow cytometry and Cell Counting Kit-8 (CCK-8) method.

2 | MATERIAL AND METHODS

2.1 | Ethics statement

All animal experiments were performed with the permission of the Animal Ethics Committee and of Second People's Hospital of Yunnan Province and in accordance with the Principles of Laboratory Animal Care. The study was conducted in accordance with the Basic & Clinical Pharmacology & Toxicology policy for experimental and clinical studies.[25] The usage of drugs was in line with the Organization for Economic Co-operation and Development (OECD) guidelines for the Testing of Chemicals. Great attempts were made to minimize the number and suffering of animals. The animals were housed in clean, comfortable and safe living conditions, and they were given sufficient water, food and nutrient substances. On the premise of not affecting the experimental results, animals were mildly anaesthetized through inhalation of isoflurane when necessary to relieve their pain.

2.2 | Animal model establishment

Ninety-five healthy female Wistar rats (250-300 g) acquired from the Experimental Animal Research Center of Second People's Hospital of Yunnan Province were housed in a specific pathogen-free animal facility in a standard 12-h dark/light cycle. A rat model with PQ-induced lung injury was established as previously reported.[22] PQ (CAS No. 1910-42-5,99%) was purchased from Sigma-Aldrich Chemical Company, while thalidomide (CAS No. 50-35-1,99%) was acquired from Changzhou Pharmaceutical Company. The concentration of 50 mg/kg was applied in this study. This concentration of PQ has been largely reported to induce lung injury.[26-29] Thalidomide has been reported to be applied at different doses in multiple diseases. For instance, 70 mg/kg of thalidomide reduced l-dopa-induced dyskinesia in rats with Parkinson's disease,[30] while 100 mg/kg of thalidomide suppressed the graft chronic rejection in a rat model of kidney transplantation,[31] reduced the paclitaxel-induced memorial impairment[32] and reduced the acute lung injury in rats.[33] In addition, thalidomide at a dose of 200 mg/kg showed protective roles

in diabetes-related disorders,[34,35] and 50 mg/kg was also found to relieve neuronal pain and spatial memory deficit in rats.[36,37] Here, we used 60 mg/kg as a moderate concentration for thalidomide administration in rats.

Rats were numbered by weight and randomly allocated into 9 groups: blank group (n = 10, oral gavage of 1 mL normal saline solution); control group (n = 10, oral gavage of 1 mL normal saline solution, followed by oral gavage of 60 mg/kg thalidomide once per day, and 6 days a week for 2 weeks); model group (n = 15, once oral gavage of PQ at 50 mg/kg in 1 mL saline); thalidomide group (n = 10, once oral gavage of PQ at 50 mg/kg in 1 mL saline, followed by oral gavage of thalidomide at 60 mg/kg once per day, and 6 days a week for 2 weeks); delay-thalidomide group (n = 10, once oral gavage of PQ at 50 mg/kg in 1 mL saline; 72 h later, oral gavage of thalidomide at 60 mg/kg once per day, and 6 days a week for 2 weeks); negative control (NC) inhibitor group (n = 10, pre-injection of lentiviral vector (LV) of NC inhibitor, followed by PQ and thalidomide treatments from the second day); miR-141 inhibitor group (n = 10, pre-injection of LV of miR-141 inhibitor, followed by PQ and thalidomide treatments from the second day); LV-NC group (n = 10, pre-injection of LV-NC, followed by PQ and thalidomide treatments from the second day); and LV-HDAC6 group (n = 10, pre-injection of LV-HDAC6, followed by PQ and thalidomide treatments from the second day). The administration dose of LV and the controls was 200 μL in each rat at a density of 2×10^8 U/mL. The LV and the control vectors were given one time per day and constantly for a week. All LV were purchased from GenePharma Co., Ltd. On the 16th day, the animals were killed via intraperitoneal injection of overdose pentobarbital sodium (200 mg/kg). Animal death was confirmed in animals by cardiac arrest, a loss of spontaneous breath for continuous 3 minutes and loss of blinking reflex. Thereafter, the lung tissues of rats were collected for further experiments.

2.3 | Cell model establishment

Type II rat alveolar epithelial cells (RLE-6TN) purchased from American Type Culture Collection (CRL-2300, ATCC) were used. The cells were seeded in Roswell Park Memorial Institute (RPMI)-1640 supplemented with 10% foetal bovine serum at a density of 1×10^5 cells/mL and cultured at 37°C with 5% CO_2 with the medium refreshed every two days. The cells were passaged at a ratio of 1:3 once the confluence reaching 80%.

A PQ-treated cell model was constructed as guided by a previous report.[24] In detail, cells were assigned into 10 groups: blank group [cells in 0.8 mL medium were treated with 1.2 mL phosphate-buffered saline (PBS)]; control group [cells in 0.8 mL medium were treated with 0.8 mL PBS and 0.4 mL thalidomide (2.5 mmol/L)]; model group [cells in 0.8 mL medium were treated with 0.8 mL PBS and 0.4 mL PQ (500 μmol/L)]; thalidomide group [cells were pre-treated with 0.4 mL PBS and 0.4 mL thalidomide for 2 hours, respectively, and then treated with 0.4 mL PQ (500 μmol/L)]; NC inhibitor group (cells were pre-transfected with NC inhibitor for 24 hours, followed by the same treatments in the thalidomide group); miR-141 inhibitor group (cells were pre-transfected with miR-141 inhibitor for 24 hours, followed by the same treatments in the thalidomide group); LV-NC group (cells were pre-transfected with LV-NC for 24 hours, followed by the same treatments in the thalidomide group); and LV-HDAC6 group (cells were pre-transfected with LV-HDAC6 for 24 hours, followed by the same treatments in the thalidomide group); dimethyl sulphoxide (DMSO) group (cells were pre-treated with DMSO for one hour, followed by the same treatments in the model group), N-acetylcysteine (NAC) group (cells were pre-treated with NAC for one hour, followed by the same treatments in the model group). All transfection was performed using a Lipofectamine 2000 kit (Invitrogen) in accordance with the kit instructions.

2.4 | Determination of the ratio of W/D weight of lung tissues

After euthanasia, the upper right lobes in rat lungs were collected and washed by sterile saline for three times. Then, the wet weight was confirmed after absorption of the remaining water using filter papers. The tissues were further dried at 80°C for 48 hours, and then, the dry weight was evaluated. The ratio of W/D weight of each rat was detected and the average W/D value in each group was calculated to assess the lung oedema.

2.5 | HE staining

The lung tissues of each group of rats were collected, fixed in 10% formalin buffer, embedded in paraffin and cut into sections (2 μm). The sections were dewaxed and stained with haematoxylin (H3136) and eosin (232954, Sigma-Aldrich) for 2 hours, and then observed under a microscope.

The inflammation in lung tissues, according to the HE staining, was scored by a group-blinded pathologist as previously described.[38] The scoring criteria were as follows: 0 = no inflammation; 1 = mild inflammation with the presence of inflammatory lesions in the walls of bronchi or blood vessels, or the alveolar septum; 2 = moderate inflammation with the presence of patchy or local inflammation in the walls of bronchi or blood vessels, or the alveolar septum;

3 = severe inflammation with the presence of diffuse inflammatory cells in the walls of bronchi or blood vessels, or the alveolar septum.

2.6 | Evaluation of oxidative stress injury

ELISA kits purchased from Jiancheng Bioengineering Institute (Nanjing, Jiangsu, China) were used to determine the expression of reactive oxygen species (ROS, No. E004-1-1) and malondialdehyde (MDA, No. A003-2). The middle lobe of the rat right lung was collected, washed in cold PBS, sliced and placed in a homogenizer tube. Phosphate and carbonate isotonic solution (0.05 M) was used as the homogenate medium. The tissues were fully grinded, and then, the homogenate was centrifuged at 1000 *g* for 10-15 min to collect the supernatant. The corresponding reagents were prepared as per the kit's instructions, and the relative expression of ROS and MDA was determined by chemiluminescence and thiobarbituric acid methods, respectively.

2.7 | Western blot analysis

Total protein from tissues or cells was extracted using the radio-immunoprecipitation assay (RIPA) lysis buffer containing proteinase inhibitor (Solarbio Science & Technology Co. Ltd.). Protein concentration was determined using a Pierce™ bicinchoninic acid kit (No. 23227, Thermo Fisher Scientific). Then, the protein samples were run on sodium dodecyl sulphate polyacrylamide gel electrophoresis and transferred on polyvinylidene fluoride membranes (EMD Millipore). Next, the membranes were blocked in 5% non-fat milk and incubated with the primary antibodies (see below) at 4°C overnight, and then with the corresponding secondary antibodies at room temperature for 2 hours. After that, the membranes were soaked in enhanced chemiluminescence reagent (WBKLS0100, EMD) in the dark and developed after light exposure. The protein bands were analysed, and the ratio of grey value of target bands to internal control band (GAPDH) was calculated as the relative protein expression. Three independent experiments were performed. The primary antibodies were B-cell lymphoma-2 (Bcl-2, 1:1000, MAB8272, rndsystems), Bcl-2-associated X (Bax, 1:1000, #2772, Cell Signaling Technology), interleukin-6 (IL-6, 1:1000, ab208113, Abcam Inc), tumour necrosis factor-α (TNF-α, 1:1000, ab6671, Abcam), basic fibroblast growth factor (bFGF, 1:1000, sc-365106, Santa Cruz Biotechnology), GAPDH (1:10 000, ab181602, Abcam), IκBα (1:1000, #4814, CST), pIκBα (Ser32/36, 1:1000, #9246, CST), NF-κB-p65 (1:1000, #6956, CST) and pNF-κB p65 (Ser536, 1:1000, #3033, CST), while the secondary antibodies used were goat anti-rabbit immunoglobulin G (IgG) H&L (HRP) (1:10 000, ab6721, Abcam) and goat anti-mouse IgG H&L (HRP, 1:10 000, ab205719, Abcam).

2.8 | CCK-8 method

A total of 2×10^3 exponentially growing RLE-6TN cells were evenly seeded on a 96-well plate (96 μL per well). The plate was placed in the incubator for cell adherence. Next, each well was loaded with 10 mL CCK-8 solution (C0037, Beyotime Biotechnology Co., Ltd.) for another 2-hour incubation at 37°C with 5% CO_2. Then the optical density (OD) value of each well was determined at 450 nm.

2.9 | ROS elimination experiments

ROS scavenger NAC (CAS No. 616-91-1, purity >98%) was acquired from MedChemExpress. The RLE-6TN cells were pre-treated with 5 mmol/L NAC for 1 h followed by PQ exposure, and then, the cytotoxicity in cells was determined by the CCK-8 assay. Cells pre-treated with DMSO were set as control.

2.10 | Flow cytometry

An Annexin V fluorescein isothiocyanate (FITC)/propidium iodide (PI) kit (V13242, Thermo Fisher Scientific) was used for apoptosis measurement. The 1× Annexin binding buffer was prepared as per the kit protocol. Cells after transfection were collected using the PI stock solution and washed with cold PBS. Next, the cells were centrifuged to discard the supernatant, and resuspended in the 1× Annexin binding buffer, followed by the treatment of annexin V FITC and PI working solutions. After a 15-minute incubation at room temperature, the cells were further mixed with the binding buffer on ice. The apoptosis of cells was analysed using the Cell-Quest software (Becton Dickinson) and a flow cytometer (FACSCalibur, BD).

2.11 | miRNA microarray analysis

SurePrint Rat miRNA Microarrays purchased from Agilent Technologies were used. In brief, total RNA from tissues was collected using a miRNeasy FFPE Kit (Qiagen, GmbH) or a Recover All Total Nucleic Acid Isolation Kit (Thermo Fisher Scientific). The RNA quality was examined using the Agilent 2100 Bioanalyzer Eukaryote Total RNA Nano or Pico assay. Next, the RNA was labelled, hybridized and washed, and the microarray chips were scanned as per the protocol manuals.

The differentially expressed miRNAs between the model and thalidomide groups were screened.

2.12 | RT-qPCR

Total RNA from tissues or cells was extracted using the TRIzol reagent (Invitrogen) and transcribed into complementary DNA (cDNA) using a Reverse Transcription Kit (No.4374966, Invitrogen). Next, real-time qPCR was performed using a Universal SYBR Green Master (Vazyme Biotech) on an ABI 7500 Real-Time qPCR System according to the protocols. Table 1 lists the primer sequences in which 5S and GAPDH served as the internal references. Relative gene expression was determined using the $2^{-\Delta\Delta CT}$ method with three independent experiments carried out.

2.13 | RNA immunoprecipitation (RIP) analysis

A Magna RIP Kit (17-710, Merck Millipore) was applied. In brief, the RLE-6TN cells were harvested and lysed in RIP lysis buffer. After that, 100 μL cell extract was cultivated with RIP buffer supplemented with magnetic beads conjugated with rat anti-Ago2 with anti-IgG served as NC. The protein was detached by proteinase K, and then, the precipitated RNA was purified and collected for RT-qPCR to evaluate the HDAC6 and miR-141 expression in precipitates.

2.14 | Dual-luciferase reporter gene assay

The 293T cells (CRL-11268, ATCC) used for transfection were incubated in 24-well plates. The binding site between miR-141 and HDAC6 was predicted on StarBase (http://starbase.sysu.edu.cn/). Subsequently, the cDNA fragment containing the putative miR-141 binding site was amplified and inserted into pGL3 vectors to construct HDAC6 wild-type (WT) vector. The corresponding HDAC6 mutant type (MT) vector was constructed using a Fast Change Site-Directed Mutagenesis Kit (Agilent, Roseville City, CA, USA). The constructed WT and MT vectors were co-transfected using either miR-141 mimic or mimic control into 293T cells. Forty-eight hours later, the relative luciferase activity was examined on a luciferase reporter gene assay (Promega).

TABLE 1 Primer sequences in RT-qPCR

Gene	Primer sequence (5'-3')
miR-141	F: TCCATCTTCCAGTGCAGTGT
	R: GAACATGTCTGCGTATCTC
HDAC6	F: GCACGCTGTCTCATCCTACCT
	R: CCCGAGTTTTCATCTTTTCTGTGTG
5S	F: TGGGTTCATTTCTGGGTCTT
	R: GGATGGGAGACCGCCTGGGAATAC
GAPDH	F: TCTCTGCTCCTCCCTGTTC
	R: ACACCGACCTTCACCATCT

Abbreviations: F, forward; GAPDH, glyceraldehyde-3-phosphate dehydrogenase; HDAC6, histone deacetylase 6; R, reverse; RT-qPCR, reverse transcription quantitative polymerase chain reaction.

2.15 | Statistical analysis

SPSS 22.0 (IBM Corp.) was used for data analysis. Data were collected from at least three independent experiments and presented as mean ± standard error of the mean (SEM). Measurement data were compared using the unpaired *t* test (for 2 groups) and one-way or two-way analysis of variance (ANOVA) followed by Tukey's multiple comparison test (for more than 2 groups). *p* values were obtained from two-tailed tests, and $P < .05$ was considered to show statistical significance.

3 | RESULTS

3.1 | Thalidomide protects rats against PQ-induced lung injury

The rats presented significant poisoning symptoms including an increased respiratory rate, mouth breathing and nasal flaring within 72 hours after PQ exposure, and the food intake of rats was notably reduced. Within 14 days, 4 rats in the model group died, while the rats further administered with thalidomide were all alive and the respiratory distress of rats was alleviated. In addition, compared to the timely treatment of thalidomide, delayed administration of thalidomide (72 hours after PQ exposure) led to severe symptoms in rats, though these rats showed better conditions than those without thalidomide treatment. Next, the W/D weight ratio of rat lung was evaluated (Figure 1A). There was no major difference between rats in the control and blank groups, but the W/D weight ratio was notably increased in model rats. Timely thalidomide treatment reduced the PQ-induced oedema in rat lung tissues, but the alleviating effects of thalidomide were reduced when it was belatedly administered. These results indicated that thalidomide administration alone has no effect on oedema changes, while it, especially with a timely administration, can reduce the oedema induced by PQ. Thereafter, the lung tissue sections were collected for HE staining (Figure 1B). The control rats treated with thalidomide alone showed no significant differences compared

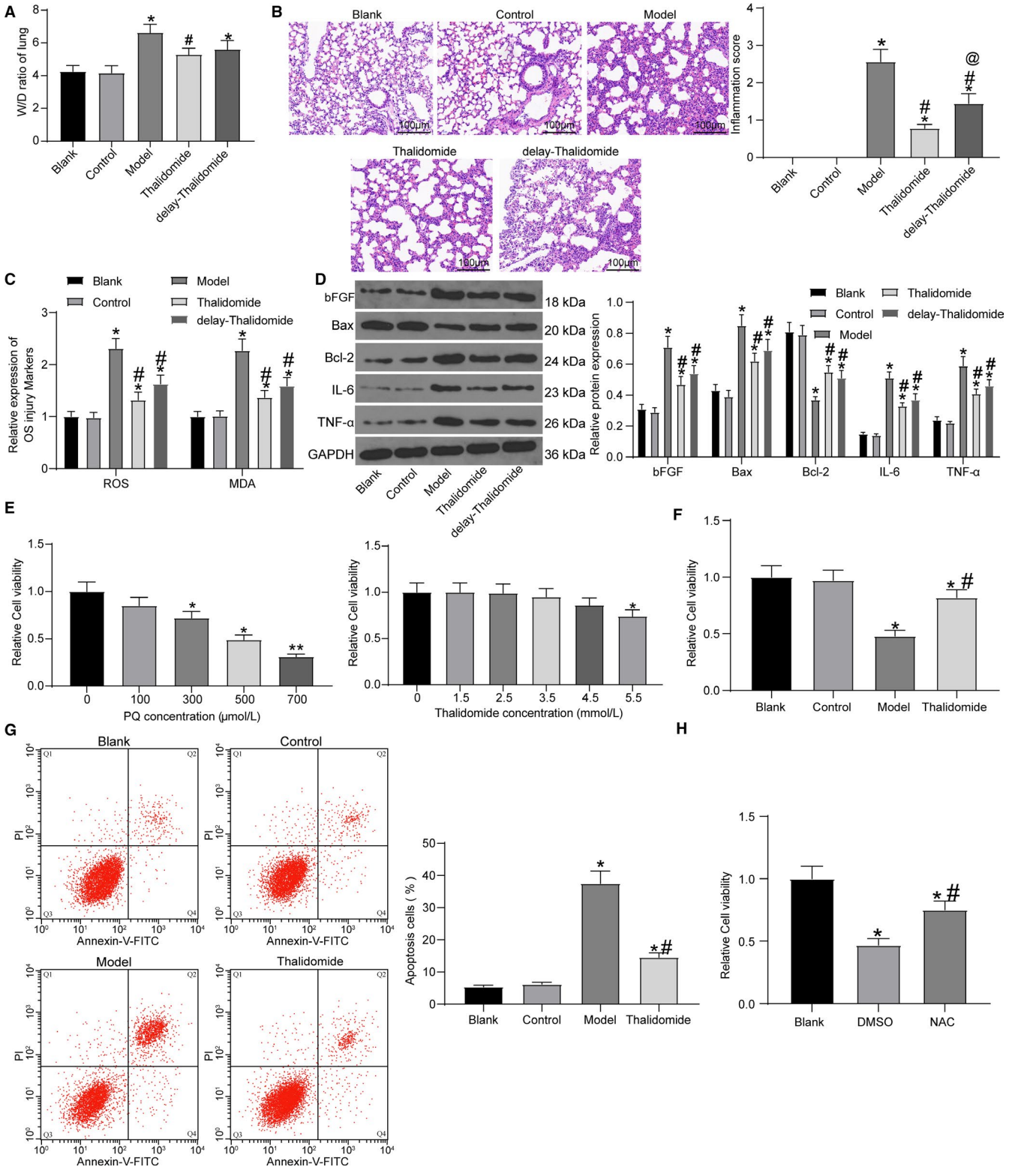

to the blank ones, indicating that thalidomide administration alone, at this concentration, showed little impact on rat lungs. However, significant lung injury with oedema, ecchymosis and inflammatory infiltration was observed in model rats, and the inflammatory score was highest in this group. Again, the PQ-induced symptoms were relieved by thalidomide, though there remained a few oedema fluid and inflammatory cells in rat lungs. The inflammatory score was higher in the delay-thalidomide group compared to the thalidomide group. In addition, the ELISA results showed that the levels of ROS and MDA were notably increased in model rats but reduced in the thalidomide group. Still, the ROS and MDA levels showed

FIGURE 1 Thalidomide protects rats against PQ-induced lung injury. (A) W/D weight ratio to reflect oedema in lungs of rats in the blank, control, model, thalidomide and delay-thalidomide groups (n = 10 in each group); (B) representative images for the histopathological changes in rat lung tissues detected by HE staining and the inflammatory score determined by a pathologist (n = 10 in each group; one-way ANOVA; $^{*}P < .05$ vs blank group; $^{\#}P < .05$ vs model group; $^{@}P < .05$ vs thalidomide group); (C) levels of ROS and MDA in rat lung tissues determined by ELISA kits (n = 10 in each group, two-way ANOVA, $^{*}P < .05$ vs blank group, $^{\#}P < .05$ vs model group); (D) levels of apoptosis-related factors (Bax and Bcl-2), fibrosis-related factor (bFGF) and inflammatory cytokines (IL-6 and TNF-α) determined by Western blot analysis (n = 10 in each group; representative images are presented; two-way ANOVA, $^{*}P < .05$ vs blank group, $^{\#}P < .05$ vs control group); (E) viability of RLE-6TN cells after different concentrations of thalidomide and PQ treatment determined by the CCK-8 method (one-way ANOVA, $^{*}P < .05$, $^{**}P < .01$ vs 0 h), (F) viability of RLE-6TN cells after thalidomide and PQ treatment determined by the CCK-8 method (one-way ANOVA, $^{*}P < .05$ vs blank group, $^{\#}P < .05$ vs model group); (G) representative images for the apoptosis of each group of cells determined by flow cytometry (one-way ANOVA, $^{*}P < .05$ vs blank group, $^{\#}P < .05$ vs model group); (H) involvement of ROS in PQ-induced cytotoxicity in cells determined by EOS elimination assay (one-way ANOVA, $^{*}P < .05$ vs blank group, $^{\#}P < .05$ vs control group). Data are expressed as mean ± SEM from three independent experiments. The representative images are presented

no major difference between the blank and control groups, but the levels were higher in the delay-thalidomide group than that in the thalidomide group (Figure 1C). Western blot analysis was further performed to determine the levels of apoptosis-related factors Bax and Bcl-2, the pro-inflammatory cytokines IL-6 and TNF-α, and the fibrosis-related factor bFGF in rat lung tissues. It was found that the levels of Bax, IL-6, TNF-α and bFGF were increased in model rats, while these changes were blocked by the further administration of thalidomide. An early administration of thalidomide showed better effects than a late one (Figure 1D). Collectively, these results indicated that thalidomide alone has no significant impact on lung damage in rats, while it reduces the PQ-induced cell apoptosis, inflammation and fibrosis in rat lung tissues. To reduce the pain in animals, timely thalidomide administration was introduced in rats in the subsequent experiments.

The functions of PQ and thalidomide on cells were evaluated as well. In a pre-experiment, we treated the RLE-6TN cells with different doses of PQ (0-700 μmol/L) and thalidomide (0-5.5 mmol/L), and then, the viability of cells was determined by the CCK-8 assay (Figure 1E). As expected, PQ suppressed the viability of cells. A dose of 500 μmol/L PQ reduced the cell viability by half. In terms of thalidomide, it was found that a low concentration of thalidomide had little effect on the viability of cells. But when the concentration of thalidomide exceeded 2.5 mmol/L, the viability of cells started to decrease. Therefore, 500 μmol/L of PQ and 2.5 mmol/L of thalidomide were used to treat the cells in in vitro experiments. According to the CCK-8 method (Figure 1F), it was found that the viability of cells between the blank (PBS treatment) and control (thalidomide administration) groups had no major difference, but that was notably decreased in the model group while increased in the thalidomide group. Likewise, a flow cytometry was used to measure apoptosis in cells (Figure 1G), which identified an increase in cell apoptosis in the model group, while this increase was blocked by thalidomide treatment. Again, there was little difference in cell apoptosis between the blank and control groups.

An ROS elimination experiment was further performed to examine the relevance between oxidative stress and the PQ-induced damage in cells. The RLE-6TN cells were pretreated with NAC (5 mM) or DMSO for an hour and then exposed to PQ, and cells without any treatment were set as blank control. The CCK-8 assay found that elimination of ROS notably reduced the toxicity of PQ in cells (Figure 1H). Collectively, these results suggested that administration of thalidomide alone has no impact on lung injury or cell damage, but it can protect rat lungs and RLE-6TN cells from PQ-induced damage.

3.2 | miR-141 upregulation is responsible for the protection of thalidomide against PQ-induced lung injury

Following the findings above, we further probed the possible molecules involved. A miRNA microarray was performed using the lung tissues from three rats in the model and thalidomide groups. The top 10 differentially expressed miRNAs are presented in Figure 2A. miR-141, identified as the mostly changed one, was selected as the subject of this study.

Thereafter, miR-141 expression in lung tissues of each group of rats was determined. The RT-qPCR results showed that compared to the blank group, miR-141 expression was increased in the control group while decreased in the model and thalidomide groups (Figure 2B), indicating miR-141 was reduced by PQ treatment while increased following independent thalidomide treatment. Thereafter, the miR-141 inhibitor or the NC inhibitor was delivered into rats before the original PQ and thalidomide co-treatment. It was found that the W/D weight ratio of rat lungs was increased after miR-141 inhibitor administration (Figure 2C). The RT-qPCR result identified a successful downregulation of miR-141 after miR-141 inhibitor administration (Figure 2D), indicating the miR-141 inhibition blocked the reducing roles of thalidomide against PQ-induced lung oedema. Again, according to the HE staining results (Figure 2E), an aggravation in oedema

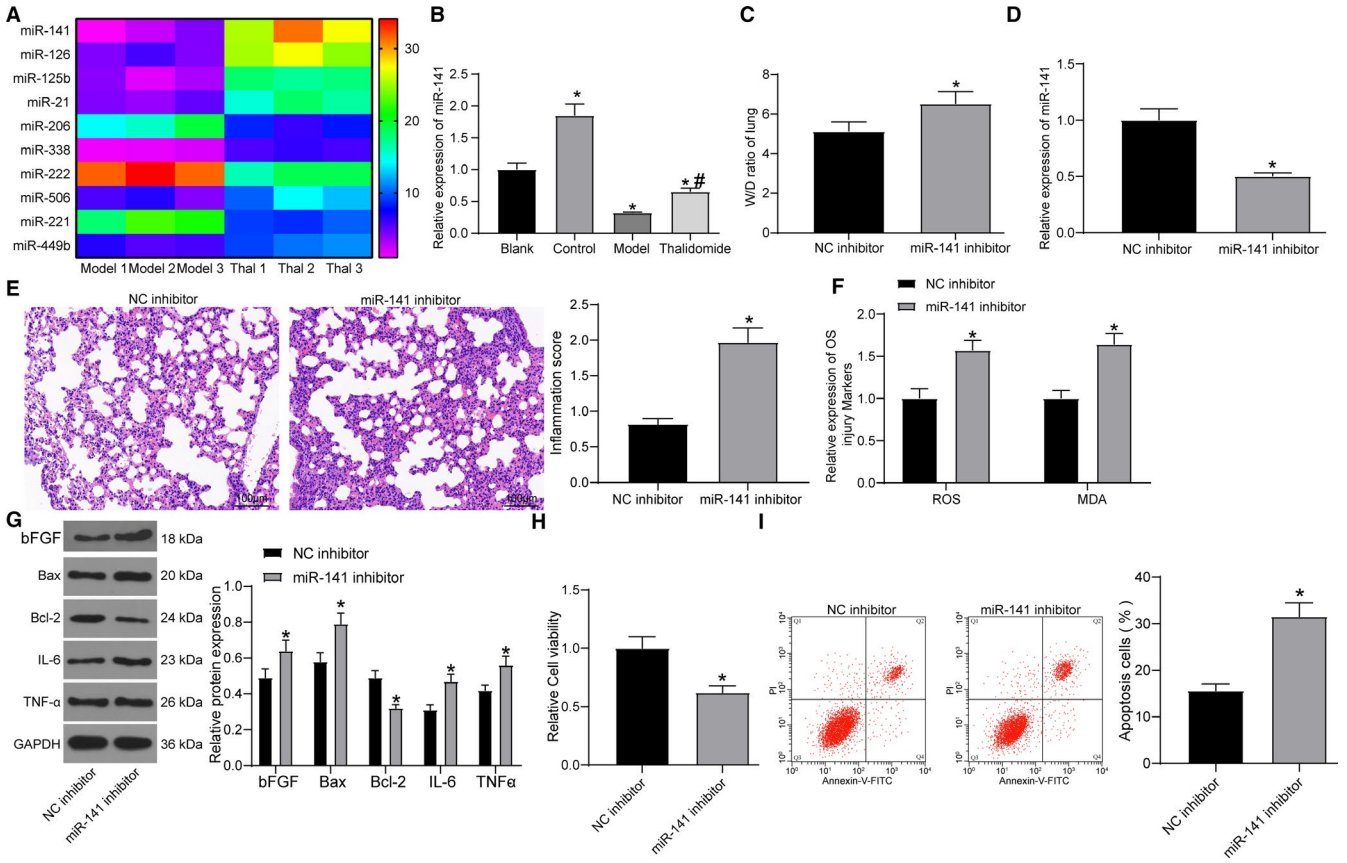

FIGURE 2 miR-141 upregulation is responsible for the protection of thalidomide against PQ-induced lung injury. (A) differentially expressed miRNAs between the rat lung tissues from the model group and the thalidomide group screened using microarray analysis (n = 3 in each group); (B) miR-141 expression in lung tissues from each group of rats determined by RT-qPCR (n = 10 in each group; one-way ANOVA, $^*P < .05$); (C) W/D weight ratio in rat lung tissues following miR-141 inhibitor treatment (n = 10 in each group, unpaired t test,$^*P < .05$ vs NC inhibitor); (D) miR-141 expression following miR-141 inhibitor or the NC treatment determined by RT-qPCR (n = 10 in each group, unpaired *t* test,$^*P < .05$, miR-141 inhibitor vs NC inhibitor); (E) representative images for the histopathological changes in rat lung tissues detected by HE staining and the inflammatory score determined by a pathologist (n = 10 in each group; unpaired *t* test,$^*P < .05$ vs NC inhibitor); (F) levels of ROS and MDA in rat lung tissues after miR-141 inhibitor or NC treatment determined by ELISA kits (n = 10 in each group; two-way ANOVA, $^*P < .05$ vs NC inhibitor); (G) levels of apoptosis-related factors (Bax and Bcl-2), fibrosis-related factor (bFGF), inflammatory cytokines (IL-6 and TNF-α) after miR-141 inhibitor or NC treatment determined by western blot analysis (n = 10 in each group, two-way ANOVA, $^*P < .05$ vs NC inhibitor group); (H) viability of RLE-6TN cells after miR-141 inhibitor or NC treatment determined by CCK-8 treatment (unpaired *t* test, $^*P < .05$ vs NC inhibitor group); (I) apoptosis rate of each group of cells determined by flow cytometry (unpaired *t* test, $^*P < .05$ vs NC inhibitor). Data are expressed as mean ± SEM from three independent experiments. The representative images are presented

and in inflammatory infiltration was observed in lung tissues after miR-141 inhibitor transfection, and the inflammatory score was increased. The ELISA results (Figure 2F) further revealed an increase in ROS and MDA expression after miR-141 inhibitor administration. Also, downregulation of miR-141 decreased the expression of Bcl-2 while increased the levels of Bax, bFGF, IL-6 and TNF-α in rat lung tissues (Figure 2G). These results implicated that downregulation of miR-141 blocks the protective effects of thalidomide on PQ-induced lung damage.

Likewise, miR-141 inhibitor or the control was pre-transfected into RLE-6TN cells prior to PQ and thalidomide treatment. Then, the CCK-8 assay found that the viability of cells increased by thalidomide was further suppressed by miR-141 inhibitor (Figure 2H). In addition, the anti-apoptotic role of thalidomide in PQ-induced cells was counteracted by miR-141 inhibitor (Figure 2I).

3.3 | miR-141 targets HDAC6

Data on Starbase suggested HDAC6 as a potential target of miR-141 (Figure 3A). HDAC6 has been noted to be closely linked to oxidative stress in injury progression.[17] We then speculated that HDAC6 is possibly regulated by miR-141 and leads to lung injury development. We then detected HDAC6 expression in lung tissues of each group of rats using RT-qPCR. The results identified that compared to the

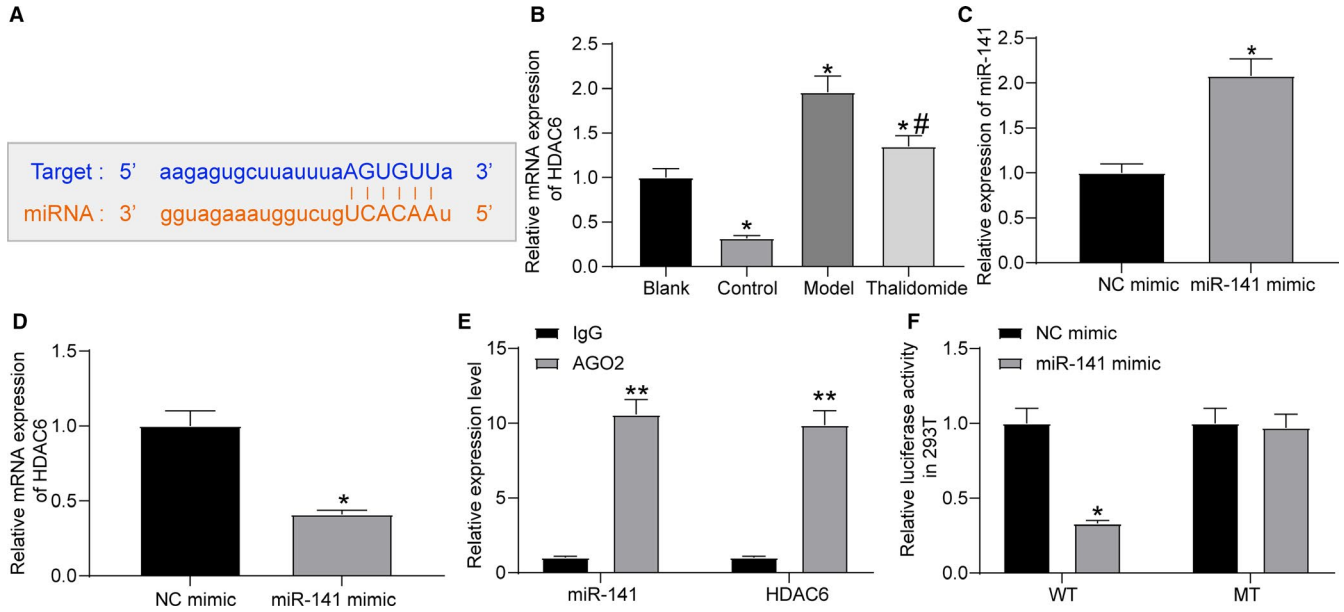

FIGURE 3 miR-141 targets HDAC6. A, putative binding site between miR-141 and HDAC6 predicted on StarBase (http://starbase.sysu.edu.cn/); B, HDAC6 expression in rat lung tissues detected by RT-qPCR (one-way ANOVA, $^{*}P < .05$ vs blank group, $^{\#}P < .05$ vs model group); C, miR-141 expression in RLE-6TN cells after miR-141 mimic or mimic control transcription detected by RT-qPCR (unpaired t test, $^{*}P < .05$ vs NC mimic group); D, mRNA expression of HDAC6 in cells after miR-141 mimic transfection measured by RT-qPCR (unpaired t test; $^{*}P < .05$ vs NC mimic group); E-F, binding relationship between miR-141 and RLE-6TN validated through a RIP assay (E, two-way ANOVA, $^{**}P < .01$ vs IgG group) and a luciferase assay (F, two-way ANOVA; $^{*}P < .05$ vs NC mimic group). Data are expressed as mean ± SEM from three independent experiments

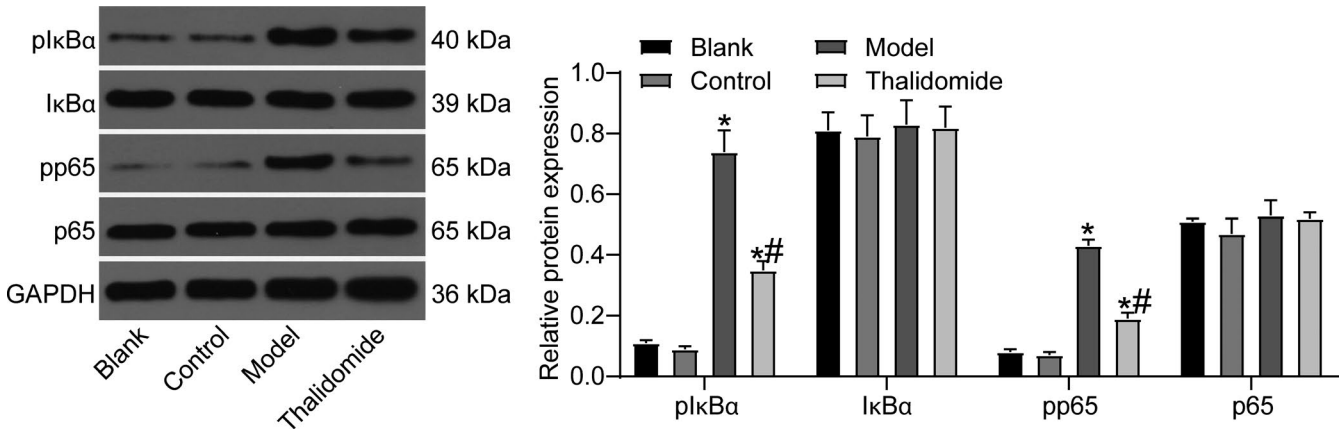

FIGURE 4 Thalidomide inhibits PQ-induced activation of the IκBα-NF-κB signalling pathway. Phosphorylation of IκBα and NF-κB p65 in rat lung tissues determined by Western blot analysis (two-way ANOVA, $^{*}P < .05$ vs blank group, $^{\#}P < .05$ vs model group). Data are expressed as mean ± SEM from three independent experiments. The representative images are presented

blank group, HDAC6 expression was notably suppressed in the control group but increased in the thalidomide and model groups, especially in the latter one. Compared to the model group, HDAC6 expression was reduced as well (Figure 3B).

To validate the correlation between miR-141 and HDAC6 expression, miR-141 mimic was administered in RLE-6TN cells, after which the miR-141 expression was successfully increased according to RT-qPCR (Figure 3C). Thereafter, we found HDAC6 expression was notably suppressed by miR-141 mimic (Figure 3D). A RIP assay was further performed, which found enrichments of miR-141 and HDAC6 in the compounds precipitated by anti-AGO2 (Figure 3E). In addition, a dual-luciferase assay was conducted, which identified a decline in luciferase activity in cells co-transfected with miR-141 mimic and HDAC6-WT vector (Figure 3F), while cells transfected with MT vector or miR-141 mimic control showed no changes in luciferase activity.

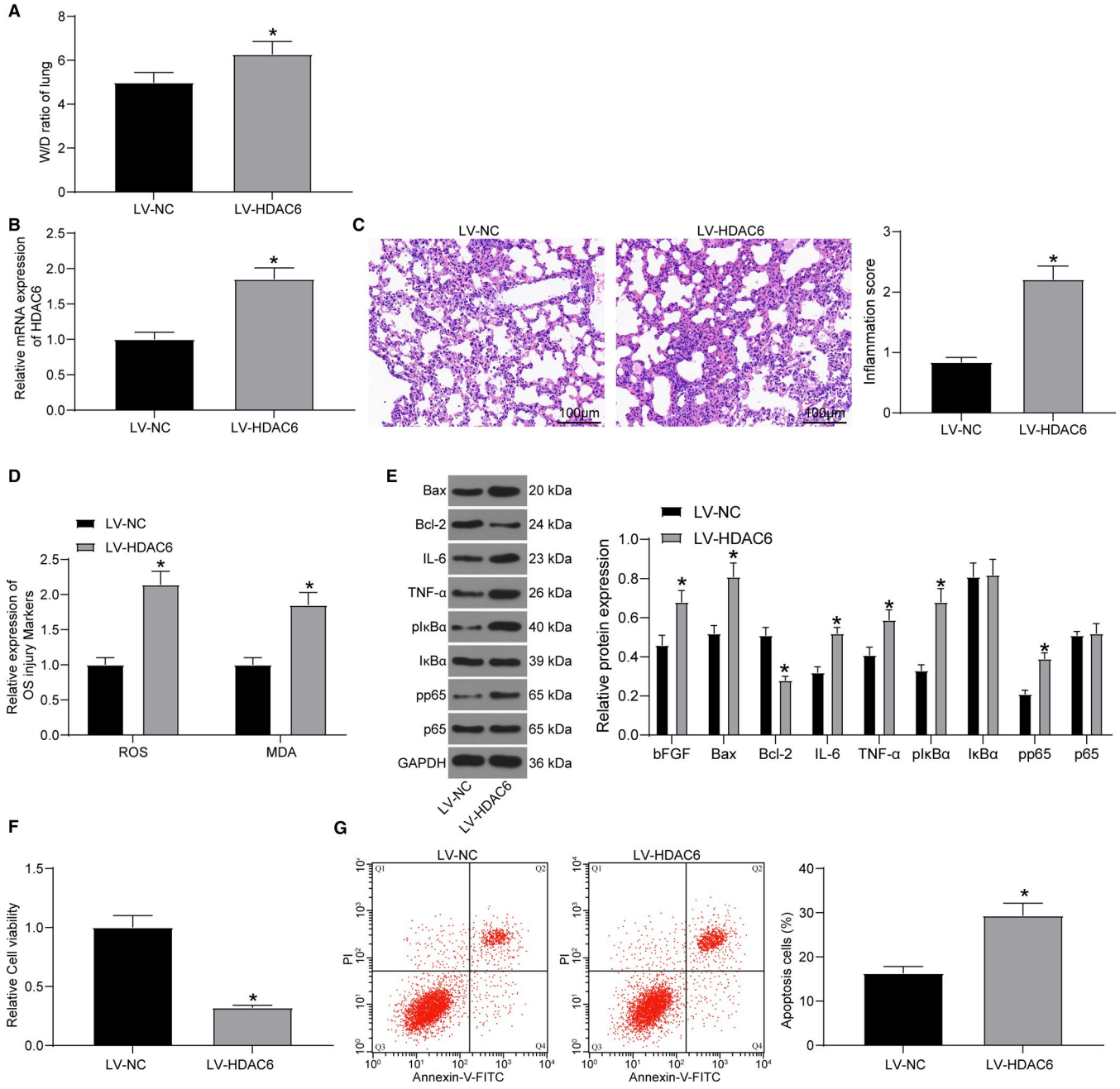

FIGURE 5 Overexpression of HDAC6 blocks the protective roles of thalidomide. (A) W/D weight ratio of rat lung tissues after LV-HDAC6 transfection (n = 10 in each group, unpaired *t* test, **P* < .05 vs LV-HDAC6 group); (B) mRNA expression of HDAC6 in rat lung tissues determined by RT-qPCR (n = 10 in each group, unpaired t test, **P* < .05 vs LV-HDAC6 group); (C) pathological injury in rat lung tissues evaluated by HE staining (n = 10 in each group, unpaired t test, **P* < .05 vs LV-HDAC6 group); (D) levels of ROS and MDA in tissues determined by ELISA kits (n = 10 in each group, two-way ANOVA, **P* < .05 vs LV-HDAC6 group); (E) protein levels of Bcl-2, Bax, bGFG, IL-6 and TNF-α, as well as phosphorylation of IκBα and NF-κB p65 in lung tissues determined using western blot analysis (n = 10 in each group; two-way ANOVA, **P* < .05 vs LV-HDAC6 group); (F) viability of RLE-6TN cells measured by CCK-8 method (unpaired *t* test, **P* < .05); (G) apoptosis rate of RLE-6TN cells detected by flow cytometry (unpaired *t* test, **P* < .05 vs LV-HDAC6 group). Data are expressed as mean ± SEM from three independent experiments. The representative images are presented

3.4 | Thalidomide inhibits PQ-induced activation of the IκBα-NF-κB signalling pathway

Phosphorylation of IκBα and NF-κB p65 was measured through Western blot analysis (Figure 4). No notable difference was found between the blank and control groups, while compared to the blank group, the phosphorylation extents of IκBα and NF-κB p65 in rat lung tissues were increased in the blank and model groups, indicating that PQ activated the IκBα-NF-κB pathway. Again, though the activation of this signalling was increased in the thalidomide

group as relative to the blank one, the phosphorylation of IκBα and NF-κB p65 was significantly reduced when compared to that in the model group.

3.5 | Overexpression of HDAC6 blocks the protective roles of thalidomide

To further confirm the involvement of HDAC6 downregulation in the protective roles of thalidomide and miR-141, rescue experiments were performed where rats or cells were pre-treated with LV-HDAC6 prior to PD and thalidomide administrations. In rat lung tissues, it was found that the W/D weight ratio was increased after LV-HDAC6 delivery (Figure 5A), and a significant increase in HDAC6 expression was identified according to RT-qPCR (Figure 5B). The HE staining results presented that the pathological injury in rat lung tissues was aggravated and the inflammatory score was increased (Figure 5C). The ELISA results showed the levels of oxidative stress-related factors ROS and MDA were increased following HDAC6 upregulation (Figure 5D). The Western blot analysis results exhibited increased levels of Bax, bFGF, IL-6 and TNF-α while decreased level of Bcl-2 in lung tissues after LV-HDAC6 administration. In addition to this, the phosphorylation of IκBα and NF-κB p65 was increased as well (Figure 5E). In RLE-6TN cells pre-transfected with LV-HDAC6, it was found that the viability of cells was decreased upon HDAC6 overexpression (Figure 5F). Correspondingly, apoptosis rate of cells was increased following HDAC6 upregulation according to the flow cytometry (Figure 5G).

4 | DISCUSSION

Clinically, there remains no available medical treatment for PQ poisoning except minimizing its absorption and struggling to prevent organ failure. PQ concentration increases continuously within the lungs in the first hours following PQ ingestion in spite of decreasing PQ levels in plasma,[6] predisposing lung as a major organ at risk following PQ exposure. The pathological presentations of PQ intoxication are acute pulmonary injury followed by rapid development of fibrosis and collagen accumulation.[4] In this paper, we validated that thalidomide is capable of alleviating lung injury induced by PQ by suppressing inflammatory responses, oxidative stress, fibrosis and cell death with the involvement of upregulation of miR-141 and downregulation of HDAC6 and the IκBα-NF-κB pathway.

Though the anti-inflammatory role of thalidomide in PQ-induced pulmonary injury has been noted in a mouse model by ameliorating the biochemical and histological presentations and the secretion of inflammatory factors,[14] the implicated mechanisms are too complicated to be fully figured out. To validate the role of thalidomide, animal and cell models treated by PQ and thalidomide were developed. Consequently, thalidomide was found to reduce lung oedema, oxidative stress (decreased ROS and MDA), inflammatory infiltration, fibrosis (bFGF) cell apoptosis (decreased Bax/Bcl-2) and production of inflammatory cytokines (IL-6 and TNF-α) in rat lung tissues. Among these changes, oxidative stress is a major consequence of PQ poisoning and a predominant cause for the subsequent alveolar epithelial cell destruction, inflammatory cell infiltration to the interstitial and alveolar spaces, and the pulmonary inflammatory and fibrosis.[8,39] Similar trends were found in a rat model with acute pancreatitis-associated lung injury, where the researchers found that thalidomide reduced adhesion molecules by reducing oxidative stress.[40] Likewise, the anti-inflammatory effect of thalidomide was also found in influenza A (H1N1) virus-induced pulmonary injury in mice by reducing the secretion of pro-inflammatory cytokines.[41] In addition, bGFG is the mostly studied fibrosis-related factor,[42,43] and PQ has been reported to enhance bGFG expression and promote fibrosis in rat lungs,[44] while thalidomide has been reported to inhibit bFGF expression in rats,[45] which was partially in line with our findings. Moreover, considering the teratogenicity[9] and potential side-effects of thalidomide, specifically, rats and cells were treated with thalidomide alone, and it was found that alone administration of thalidomide did not affect the lungs and cells.

Aberrant expression of miRNAs is closely associated with inflammatory responses including lung injury development.[46-48] A miRNA microarray analysis was applied to explore the potential molecules involved in the events mediated by thalidomide. miR-141 was identified as the mostly significantly upregulated miRNA after thalidomide treatment. Based on this finding, artificial downregulation of miR-141 was pre-introduced in rat and cell models before thalidomide and PQ treatments. It was found that the protective effects of thalidomide against PQ were blocked upon miR-141 downregulation, indicating miR-141 upregulation is responsible for the alleviating roles of thalidomide in lung injury. In a pneumonia cell model induced by LPS, upregulation of miR-141 was found to suppress cell apoptosis and inflammation response but to promote viability of MRC-5 cells.[49] Interestingly, a similar trend was found in another LPS-induced inflammatory model in WI-38 fibroblasts where miR-141 reduced inflammation through upregulation of NOX2.[16] miRNAs are well-known to primarily induce degradation of target mRNAs by direct binding. Here, we identified HDAC6 as a target of miR-141. HDAC6 inhibition has been suggested to reduce oxidative stress level to protect against rhabdomyolysis-induced kidney injury.[50] Again, in an LPS-induced acute lung injury model, inhibition of HDAC6 was reported to block activation of the inflammatory signalling and caspase-1.[51] Here,

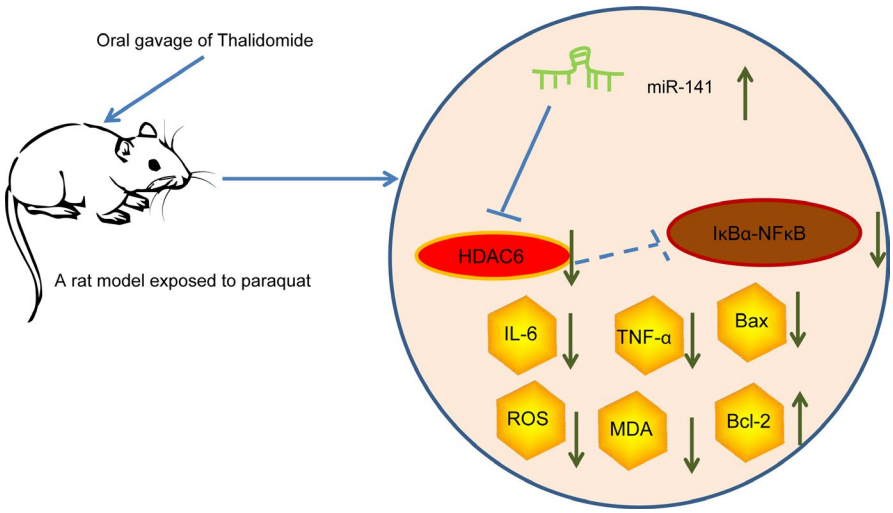

FIGURE 6 A diagram for molecular mechanism. Thalidomide increases miR-141 expression to inhibit HDAC6 expression and inactivate the IκBα-NF-κB signalling pathway, reducing inflammatory cytokine secretion (IL-6 and TNF-α), oxidative stress (ROS and MDA), fibrosis (bFGF), and cell apoptosis (Bax/Bcl-2) in lung tissues in a rat model with PQ-induced lung injury

to check whether HDAC6 inhibition participates in the mediation by thalidomide-miR-141, another rescue experiment was carried out, where we found overexpression of HDAC6 blocks the alleviating roles of thalidomide in PQ-treated cells and rats. In addition, thalidomide was found to reduce phosphorylation of IκBα and NF-κB p65 in our experiments. Still, the activation of this signalling pathway is recovered following LV-HDAC6 transfection. Activation of the NF-κB family of transcription factors, which is mainly regulated by the IκB kinases and the phosphorylation and degradation of IκBα, is of major importance in the orchestration of the inflammatory responses.[52-54] More relevantly, thalidomide was noted to mitigate acute pancreatitis-associated lung injury through suppressing TNF-α induced by NF-κB.[55] The promoting role of HDAC6 in inflammation and oxidative stress was reported involving the mitogen-activated protein kinase/NF-κB signalling pathway.[56,57] Here, we report a similar molecule involved in thalidomide-initiated protection against PQ-induced lung injury, where thalidomide suppresses the IκBα-NF-κB signalling pathway through miR-141-mediated downregulation of HDAC6.

To sum up, this study evidenced by both in vivo and in vitro experiments that thalidomide alleviates PQ-induced lung injury through suppressing inflammation, oxidative stress and cell death with the involvement of miR-141 upregulation and the following HDAC6 downregulation and IκBα-NF-κB inactivation (Figure 6). These findings may provide a better understanding of the molecular mechanisms in the anti-oxidative and anti-inflammatory effects of thalidomide. However, thalidomide is a multi-potent chemical with other functions such as induction of monocyte apoptosis[58] and anti-angiogenic property.[59] Though we found that administration of thalidomide alone did not affect the pathological changes in rats and the cells, its potential function on monocytes was not concerned. Also, due to the time and funding limits, the relevance of the anti-angiogenetic role of thalidomide to the fibrotic and injury processes of PQ was not discussed in this study. We would like to address these issues in future studies. We hope more studies will be carried out in the future to offer new ideas for lung injury treatment.

ACKNOWLEDGEMENTS

This project was supported by Key project of Kunming Science and Technology Plan: Basic and Clinical Study on Thalidomide in the Treatment of Paraquat Poisoning Lung Injury (2015-2-S-01408).

CONFLICT OF INTEREST

All authors declare that there is no conflict of interests in this study.

ORCID

Zhaoheng Lin https://orcid.org/0000-0002-6488-8147

REFERENCES

1. Yanling W, Duo G, Zuojun G, et al. Radiomics nomogram analyses for differentiating pneumonia and acute paraquat lung injury. *Sci Rep.* 2019;9(1):15029.
2. Li LR, Sydenham E, Chaudhary B, Beecher D, You C. Glucocorticoid with cyclophosphamide for paraquat-induced lung fibrosis. *Cochrane Database Syst Rev.* 2014;(8):CD008084.
3. Sun B, Chen YG. Advances in the mechanism of paraquat-induced pulmonary injury. *Eur Rev Med Pharmacol Sci.* 2016;20(8):1597-1602.
4. He F, Zhou A, Feng S, Li Y, Liu T. Mesenchymal stem cell therapy for paraquat poisoning: a systematic review and meta-analysis of preclinical studies. *PLoS One* 2018;13(3):e0194748.
5. Ryu S, Lee JM, Bae CA, Moon CE, Cho KO. Therapeutic efficacy of neuregulin 1-expressing human adipose-derived mesenchymal stem cells for ischemic stroke. *PLoS One* 2019;14(9):e0222587.
6. Gil HW, Hong JR, Jang SH, Hong SY. Diagnostic and therapeutic approach for acute paraquat intoxication. *J Korean Med Sci.* 2014;29(11):1441-1449.

7. Xu L, Xu J, Wang Z. Molecular mechanisms of paraquat-induced acute lung injury: a current review. *Drug Chem Toxicol.* 2014;37(2):130-134.
8. Blanco-Ayala T, Anderica-Romero AC, Pedraza-Chaverri J. New insights into antioxidant strategies against paraquat toxicity. *Free Radic Res.* 2014;48(6):623-640.
9. Asatsuma-Okumura T, Ito T, Handa H. Molecular mechanisms of the teratogenic effects of thalidomide. *Pharmaceuticals (Basel).* 2020;13(5). https://doi.org/10.3390/ph13050095
10. Xu M, Wang X, Xu X, et al. Thalidomide prevents antibody-mediated immune thrombocytopenia in mice. *Thromb Res.* 2019;183:69-75.
11. Guo L, Wan Z, Xu B, et al. Blockade of angiogenin by thalidomide inhibits the tumorigenesis of murine hemangioendothelioma. *Fundam Clin Pharmacol.* 2019;33(6):659-669.
12. Santana AC, Degaspari S, Catanozi S, et al. Thalidomide suppresses inflammation in adenine-induced CKD with uraemia in mice. *Nephrol Dial Transplant.* 2013;28(5):1140-1149.
13. Viswanathan P, Gupta P, Kapoor S, Gupta S. Thalidomide promotes transplanted cell engraftment in the rat liver by modulating inflammation and endothelial integrity. *J Hepatol.* 2016;65(6):1171-1178.
14. Amirshahrokhi K. Anti-inflammatory effect of thalidomide in paraquat-induced pulmonary injury in mice. *Int Immunopharmacol.* 2013;17(2):210-215.
15. Ebrahimi SO, Reiisi S, Shareef S. miRNAs, oxidative stress, and cancer: a comprehensive and updated review. *J Cell Physiol.* 2020;235:8812-8825.
16. Quan B, Zhang H, Xue R. miR-141 alleviates LPS-induced inflammation injury in WI-38 fibroblasts by up-regulation of NOX2. *Life Sci.* 2019;216:271-278.
17. Guo SD, Yan ST, Li W, et al. HDAC6 promotes sepsis development by impairing PHB1-mediated mitochondrial respiratory chain function. *Aging (Albany NY).* 2020;12(6):5411-5422.
18. Leng Y, Wu Y, Lei S, et al. Inhibition of HDAC6 activity alleviates myocardial ischemia/reperfusion injury in diabetic rats: potential role of peroxiredoxin 1 acetylation and redox regulation. *Oxid Med Cell Longev.* 2018;2018:9494052.
19. Shin NR, Kim C, Seo CS, et al. Galgeun-tang attenuates cigarette smoke and lipopolysaccharide induced pulmonary inflammation via IkappaBalpha/NF-kappaB signaling. *Molecules* 2018;23(10). https://doi.org/10.3390/molecules23102489
20. Kim DI, Kim SR, Kim HJ, et al. PI3K-gamma inhibition ameliorates acute lung injury through regulation of IkappaBalpha/NF-kappaB pathway and innate immune responses. *J Clin Immunol.* 2012;32(2):340-351.
21. Czerniczyniec A, Karadayian AG, Bustamante J, Cutrera RA, Lores-Arnaiz S. Paraquat induces behavioral changes and cortical and striatal mitochondrial dysfunction. *Free Radic Biol Med.* 2011;51(7):1428-1436.
22. Li D, Zhang XW, Jiang XQ, et al. Protective effects of thalidomide on pulmonary injuries in a rat model of paraquat intoxication. *J Inflamm (Lond).* 2015;12:46.
23. Su SD, Cong SG, Bi YK, Gao DD. Paraquat promotes the epithelial-mesenchymal transition in alveolar epithelial cells through regulating the Wnt/beta-catenin signal pathway. *Eur Rev Med Pharmacol Sci.* 2018;22(3):802-809.
24. Wu L, Cen Y, Feng M, et al. Metformin activates the protective effects of the AMPK pathway in acute lung injury caused by paraquat poisoning. *Oxid Med Cell Longev.* 2019;2019:1709718.
25. Tveden-Nyborg P, Bergmann TK, Lykkesfeldt J. Basic & clinical pharmacology & toxicology policy for experimental and clinical studies. *Basic Clin Pharmacol Toxicol.* 2018;123(3):233-235.
26. Du J, Zhu Y, Meng X, et al. Atorvastatin attenuates paraquat poisoning-induced epithelial-mesenchymal transition via downregulating hypoxia-inducible factor-1 alpha. *Life Sci.* 2018;213:126-133.
27. Marashi SM, Hosseini SF, Hosseinzadeh M, Qadir MF, Khodaei F. Ameliorative role of aspirin in paraquat-induced lung toxicity via mitochondrial mechanisms. *J Biochem Mol Toxicol.* 2019;33(9):e22370.
28. SreeHarsha N. Embelin impact on paraquat-induced lung injury through suppressing oxidative stress, inflammatory cascade, and MAPK/NF-kappaB signaling pathway. *J Biochem Mol Toxicol.* 2020;34(4):e22456.
29. Wang J, Zhu Y, Tan J, Meng X, Xie H, Wang R. Lysyl oxidase promotes epithelial-to-mesenchymal transition during paraquat-induced pulmonary fibrosis. *Mol Biosyst.* 2016;12(2):499-507.
30. Boi L, Pisanu A, Greig NH, et al. Immunomodulatory drugs alleviate l-dopa-induced dyskinesia in a rat model of Parkinson's disease. *Mov Disord.* 2019;34(12):1818-1830.
31. Zhang Y, Yang Y, Li X, Chen D, Tang G, Men T. Thalidomide ameliorate graft chronic rejection in an allogenic kidney transplant model. *Int Immunopharmacol.* 2019;71:32-39.
32. Li Z, Zhao S, Zhang HL, et al. Proinflammatory factors mediate paclitaxel-induced impairment of learning and memory. *Mediators Inflamm.* 2018;2018:3941840.
33. Chen CS, Perng WC, Chen CW, Huang KL, Wu CP, Yen MH. Thalidomide reduces lipopolysaccharide/zymosan-induced acute lung injury in rats. *J Biomed Sci.* 2004;11(5):591-598.
34. Bosco AA, Lerario AC, Santos RF, Wajchenberg BL. Effect of thalidomide and rosiglitazone on the prevention of diabetic retinopathy in streptozotocin-induced diabetic rats. *Diabetologia* 2003;46(12):1669-1675.
35. Zhang H, Yang Y, Wang Y, Wang B, Li R. Renal-protective effect of thalidomide in streptozotocin-induced diabetic rats through anti-inflammatory pathway. *Drug Des Devel Ther.* 2018;12:89-98.
36. Ding HH, Zhang SB, Lv YY, et al. TNF-alpha/STAT3 pathway epigenetically upregulates Nav1.6 expression in DRG and contributes to neuropathic pain induced by L5-VRT. *J Neuroinflammation.* 2019;16(1):29.
37. Magnusson O, Mohringe B, Thorell G, Lake-Bakaar DM. Effects of the dopamine D2 selective receptor antagonist remoxipride on dopamine turnover in the rat brain after acute and repeated administration. *Pharmacol Toxicol.* 1987;60(5):368-373.
38. Li F, Wiegman C, Seiffert JM, et al. Effects of N-acetylcysteine in ozone-induced chronic obstructive pulmonary disease model. *PLoS One* 2013;8(11):e80782.
39. Chen Y, Nie YC, Luo YL, et al. Protective effects of naringin against paraquat-induced acute lung injury and pulmonary fibrosis in mice. *Food Chem Toxicol.* 2013;58:133-140.
40. Lv P, Li HY, Ji SS, Li W, Fan LJ. Thalidomide inhibits adhesion molecules in experimental acute pancreatitis-associated lung injury. *Drug Dev Res.* 2015;76(1):24-30.
41. Zhu H, Shi X, Ju D, Huang H, Wei W, Dong X. Anti-inflammatory effect of thalidomide on H1N1 influenza virus-induced pulmonary injury in mice. *Inflammation* 2014;37(6):2091-2098.
42. Chen B, You WJ, Liu XQ, Xue S, Qin H, Jiang HD. Chronic microaspiration of bile acids induces lung fibrosis through multiple mechanisms in rats. *Clin Sci (Lond).* 2017;131(10):951-963.

43. Weng CM, Li Q, Chen KJ, et al. Bleomycin induces epithelial-to-mesenchymal transition via bFGF/PI3K/ESRP1 signaling in pulmonary fibrosis. *Biosci Rep.* 2020;40(1). https://doi.org/10.1042/BSR20190756
44. Akcilar R, Akcilar A, Simsek H, et al. Hyperbaric oxygen treatment ameliorates lung injury in paraquat intoxicated rats. *Int J Clin Exp Pathol.* 2015;8(10):13034-13042.
45. Park SJ, Kim HS, Yang HM, et al. Thalidomide as a potent inhibitor of neointimal hyperplasia after balloon injury in rat carotid artery. *Arterioscler Thromb Vasc Biol.* 2004;24(5):885-891.
46. Ferruelo A, Penuelas O, Lorente JA. MicroRNAs as biomarkers of acute lung injury. *Ann Transl Med.* 2018;6(2):34.
47. Garavelli S, De Rosa V, de Candia P. The multifaceted interface between cytokines and microRNAs: an ancient mechanism to regulate the good and the bad of inflammation. *Front Immunol.* 2018;9:3012.
48. Rogers CJ, Lukaszewicz AI, Yamada-Hanff J, et al. Identification of miRNA signatures associated with radiation-induced late lung injury in mice. *PLoS One* 2020;15(5):e0232411.
49. Tang X, Wang T, Qiu C, Zheng F, Xu J, Zhong B. Long non-coding RNA (lncRNA) CRNDE regulated lipopolysaccharides (LPS)-induced MRC-5 inflammation injury through targeting MiR-141. *Med Sci Monit.* 2020;26:e920928.
50. Shi Y, Xu L, Tang J, et al. Inhibition of HDAC6 protects against rhabdomyolysis-induced acute kidney injury. *Am J Physiol Renal Physiol.* 2017;312(3):F502-F515.
51. Liu L, Zhou X, Shetty S, Hou G, Wang Q, Fu J. HDAC6 inhibition blocks inflammatory signaling and caspase-1 activation in LPS-induced acute lung injury. *Toxicol Appl Pharmacol.* 2019;370:178-183.
52. Gasparini C, Feldmann M. NF-kappaB as a target for modulating inflammatory responses. *Curr Pharm Des.* 2012;18(35):5735-5745.
53. Jia Z, Nallasamy P, Liu D, et al. Luteolin protects against vascular inflammation in mice and TNF-alpha-induced monocyte adhesion to endothelial cells via suppressing IKappaBalpha/NF-kappaB signaling pathway. *J Nutr Biochem.* 2015;26(3):293-302.
54. Natoli G, Chiocca S. Nuclear ubiquitin ligases, NF-kappaB degradation, and the control of inflammation. *Sci Signal.* 2008;1(1):pe1.
55. Lv P, Li HY, Ji SS, Li W, Fan LJ. thalidomide alleviates acute pancreatitis-associated lung injury via down-regulation of NFkappaB induced TNF-alpha. *Pathol Res Pract.* 2014;210(9):558-564.
56. Youn GS, Lee KW, Choi SY, Park J. Overexpression of HDAC6 induces pro-inflammatory responses by regulating ROS-MAPK-NF-kappaB/AP-1 signaling pathways in macrophages. *Free Radic Biol Med.* 2016;97:14-23.
57. Zhang WB, Yang F, Wang Y, et al. Inhibition of HDAC6 attenuates LPS-induced inflammation in macrophages by regulating oxidative stress and suppressing the TLR4-MAPK/NF-kappaB pathways. *Biomed Pharmacother.* 2019;117:109166.
58. Gockel HR, Lugering A, Heidemann J, et al. Thalidomide induces apoptosis in human monocytes by using a cytochrome c-dependent pathway. *J Immunol.* 2004;172(8):5103-5109.
59. Mercurio A, Adriani G, Catalano A, et al. A mini-review on thalidomide: chemistry, mechanisms of action, therapeutic potential and anti-angiogenic properties in multiple myeloma. *Curr Med Chem.* 2017;24(25):2736-2744.

How to cite this article: Zheng F, Zhu J, Zhang W, Fu Y, Lin Z. Thal protects against paraquat-induced lung injury through a microRNA-141/HDAC6/IκBα-NF-κB axis in rat and cell models. *Basic Clin Pharmacol Toxicol*. 2021;128:334–347. https://doi.org/10.1111/bcpt.13505